SPACE CHARGE EFFECTS ON LANDAU DAMPING FROM OCTUPOLES

V. Kornilov, GSI Helmholtzzentrum, Darmstadt, Germany
O. Boine-Frankenheim, GSI Helmholtzzentrum and TU Darmstadt, Germany

INTRODUCTION

Octupole magnets are the cornerstone of the collective instability mitigation in many hadron synchrotrons, including the future SIS100 synchrotron [1] of the FAIR project [2]. The betatron tune shifts, and the tune spread, linearly increase with the octupole magnet current, and enhance Landau damping. On the other hand, a strong octupole field, as a nonlinearity, can reduce the dynamic aperture [3, 4]. This can put a restriction for the allowable octupole magnet power. Thus, a good understanding of the octupole magnet usage for Landau damping of the collective instabilities is important.

The direct space-charge can produce comparable or stronger tune shifts than the octupoles. Thus the effects of space-charge should be taken into account in a study for Landau damping due to octupoles. Space-charge can have manifold effects on Landau damping. Space-charge can cause loss of Landau damping, it can provide Landau damping, it changes the incoherent tune distribution and thus changes Landau damping in the beam.

The bunched beams are considered in this work, with the focus on the head-tail instability. Head-tail modes [5] are eigenmodes of the transverse collective bunch oscillations. Unstable head-tail modes are a major concern for high-intensity operation in ring accelerators. We consider unstable head-tail modes with different mode indices k, with the non-rigid bunch oscillations due to a finite chromaticity, even the lowest-order mode $k = 0$.

In the next section we review some properties of Landau damping in coasting beams and in bunches, the effects of octupoles and space-charge. For this discussion we consider two dispersion relations. The particle tracking simulations and the stability study method are described, followed by the results for the beam stability due to octupoles with space-charge of different strength. The results and the conclusions are discussed with the consideration of the incoherent tune distributions.

THEORY ASPECTS

The space-charge tune shift varies along the bunch,

$$\Delta Q_{\mathrm{sc}}(z) = \frac{g_\perp \lambda(z) r_p R}{4\gamma^3\beta^2\varepsilon_x}\,, \tag{1}$$

where $\lambda(z)$ is the line density, $(2\pi R)$ is the ring circumference, β and γ are the relativistic parameters, $r_p = q_{\mathrm{ion}}^2/(4\pi\epsilon_0 mc^2)$ is the classical particle radius, ε_x is the transverse rms emittance. The space-charge tune shift is negative (a tune depression), the modulus of the tune shift is different for every individual particle, depending on the transverse amplitudes and on the longitudinal position along the bunch. Equation 1 gives the maximal tune shift (for particles with small transverse amplitudes) for the position z, in a round beam. The geometric factor $g_\perp$ depends on the transverse distribution, for the Gaussian profile it is $g_\perp = 2$. The space-charge parameter is

$$q = \frac{\Delta Q_{\mathrm{sc}}(0)}{Q_s} \tag{2}$$

which is the tune shift for the rms-eqivalent K-V beam [6] ($g_\perp = 1$) in the peak of the line density, normalized by the synchrotron tune Q_s.

An octupole magnet of the strength O_3 produces the magnetic field

$$\begin{aligned} B_x &= O_3(3x^2y - y^3), \\ B_y &= O_3(x^3 - 3xy^2), \end{aligned} \tag{3}$$

which contributes to the incoherent tune shifts [3] of an octupole magnet system,

$$\begin{aligned} \Delta Q_x &= \kappa_x J_x - \kappa_{xy} J_y\,, \\ \Delta Q_y &= \kappa_y J_y - \kappa_{xy} J_x\,, \end{aligned} \tag{4}$$

where J_x, J_y are the horizontal and vertical action variables.

For a characteristic tune shift due to octupoles, we use the parameter

$$q_4 = \frac{\Delta Q_\sigma}{Q_s}, \tag{5}$$

where ΔQ_σ is the tune shift ΔQ_x of a particle with the amplitudes $a_x = \sigma_x, a_y = 0$ (σ_x is the transverse rms beam size), which corresponds to $J_x = \varepsilon_x/2, J_y = 0$.

For calculations of Landau damping due to octupole, the dispersion relation has been often used [3, 7–10],

$$\Delta Q_{\mathrm{coh}} \int \frac{1}{\Delta Q_{\mathrm{oct}} - \Omega/\omega_0} J_x \frac{\partial \psi_\perp}{\partial J_x} dJ_x dJ_y = 1. \tag{6}$$

Here, $\omega_0 = 2\pi f_0$ is the revolution frequency, the incoherent tune shift $\Delta Q_{\mathrm{oct}}(J_x, J_y)$ and the distribution function $\psi_\perp(J_x, J_y)$ are two-dimensional dependences. This represents the important role of the transverse beam profile in Landau damping. The coherent tune shift ΔQ_{coh} results from the machine impedance in the case of no tune spread, i.e. no Landau damping. The collective mode frequency Ω is the solution for the given impedance, tune spread, and the beam distribution. This is the dispersion relation for the horizontal plane, the corresponding form is for the vertical oscillations. The dispersion relation Eq. (6) has been derived for a coasting beam, or for rigid dipole oscillations in bunches, but is has been commonly used also for estimations for the higher-order head-tail modes. Landau damping due to octupoles

for non-rigid oscillations of different order modes has been recently studied in [11].

The effects of direct space-charge have been taken into account in another dispersion relation [12, 13],

$$\int \frac{\Delta Q_{\rm coh} - \Delta Q_{\rm sc}}{\Delta Q_{\rm oct} + \Delta Q_{\rm sc} - \Omega/\omega_0} J_x \frac{\partial \psi_\perp}{\partial J_x} dJ_x dJ_y = 1. \qquad (7)$$

This is also a 2d case, with the dependency $\Delta Q_{\rm sc}(J_x, J_y)$. This dispersion relation predicts an important role of nonlinear space-charge [14, 15] for Landau damping. The loss of Landau damping due to space-charge — the incoherent spectrum shifts away from the collective frequency due to linear space-charge [16–18] — is implicated in Eq. (7). This dispersion relation also correctly suggests that there is no Landau damping due to nonlinear space-charge only [16], even if the coherent frequency overlaps the incoherent tune spread. Particle tracking simulations with space-charge [16] confirmed these conclusions. However, for some $(\Delta Q_{\rm oct}+\Delta Q_{\rm sc})(J_x, J_y)$ dependencies Eq. (7) predicts an unphysical antidamping [16–18].

In the case of head-tail modes in bunches, there are additional aspects. Due to the chromatic phase advance along the bunch, already a $k = 0$ head-tail mode is not a rigid-bunch oscillation [11], the higher-order modes have more complicated longitudinal structures [5]. The synchrotron motion plays an important role, the longitudinal density profile $\lambda(z)$ creates space-charge tune shift variations along the bunch.

In contrast to the case of a coasting beam, the space-charge induced tune spread provides damping for the modes $k \neq 0$ [19–23]. Damping rates due to the tune spread produced by the longitudinal bunch density variations have been demonstrated and quantified in [22], effects of tune spreads in the longitudinal and transverse planes have been studied in [21,23]. This Landau damping can not be described by the dispersion relations Eqs. (6, 7) . A combination with the nonlinearities due to octupoles is even more complicated, which we study in this work using the particle tracking simulations.

PARTICLE SIMULATIONS WITH SPACE CHARGE AND OCTUPOLES

For the particle tracking simulations we use the particle-in-cell code PATRIC [22–24, 26] in the PIC mode. The code has been validated using the exact analytical predictions [22,25,26], for the cases with and without space-charge, for bunched and for coasting beams. Chromatic effects and the octupole fields Eq. (3) are implemented as transverse momentum kicks, uniformly distributed over the ring. A linear rf bucket is used, i.e. the effects of the rf nonlinearity are not taken into account, the synchrotron tune in the simulations of this paper is $Q_s = 0.01$. The machine and beam parameters for the simulations are inspired by the heavy ion synchrotron SIS18 [27] at GSI Darmstadt, in our simulations with the uniform focusing model. The bunch distribution is 3D Gaussian, the beam is round transversally, the resistive-wall wake $W(z) = w_0/\sqrt{z}$ is applied in the horizontal plane, in the longitudinally-sliced manner [25]. For the self-field space-charge, the self-consistent solver is used in this work. This is necessary because of changes in the beam profiles during the beam oscillations with octupoles [11]. The beam profile modifications should be correctly included into the self-consistent space-charge structure. Beam losses are involved by an aperture with the radius four times larger than the initial beam radius.

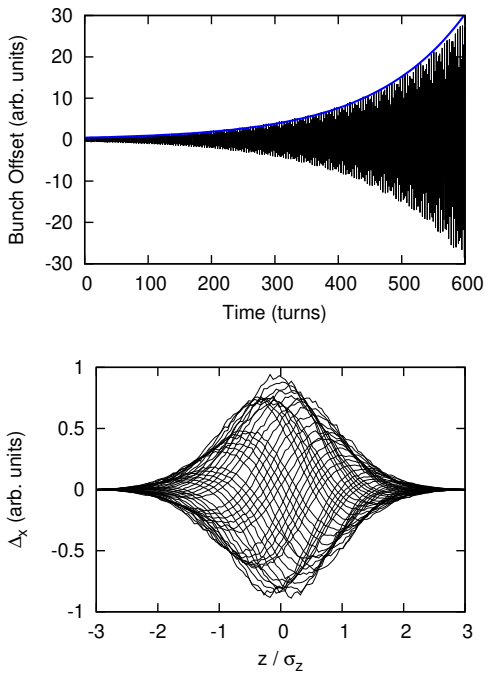

Figure 1: Example for an unstable $k = 0$ head-tail mode from a simulation without octupoles. The top plot: time evolution of the bunch offset (black line), the blue line is an exponential with the growth rate $\Gamma = 1.1 \times 10^{-3}$. The bottom plot: related offset traces along the bunch.

A simulation is started with a tiny perturbation. In the case without damping mechanism the perturbation grows into a linear instability, see Fig. 1 for an example. The amplitude increases exponentially (the blue line in Fig. 1, top) with the growth rate $\Gamma = {\rm Im}(\Delta Q_{\rm coh}) = 1.1 \times 10^{-3}$. The bottom plot in Fig. 1 shows the transverse offset overlap from this simulation, σ_z is the rms bunch length. It has a typical pattern of a $k = 0$ head-tail mode, the wiggles demonstrate that this is a non-rigid mode.

We study the head-tail modes of different order by shifting the chromaticity ξ and thus the chromaticity phase shift $\chi_b = Q_0 \xi L_b/(\eta R)$. For example, the $k = 0$ mode (Fig. 1) is the most unstable mode for $\chi_b = -1.15$ in our case. For $\chi_b = 0.55$ the most unstable mode is the $k = 1$ head-tail mode (Fig. 2, top plot), for $\chi_b = 0.88$ the most unstable mode is $k = 2$ (Fig. 2, bottom plot).

In our simulation scans we vary the octupole strength and the space-charge parameter. The wake field and the chromaticity stay fixed for every head-tail mode. As a result, the mode drive does not change within the scans. The growth

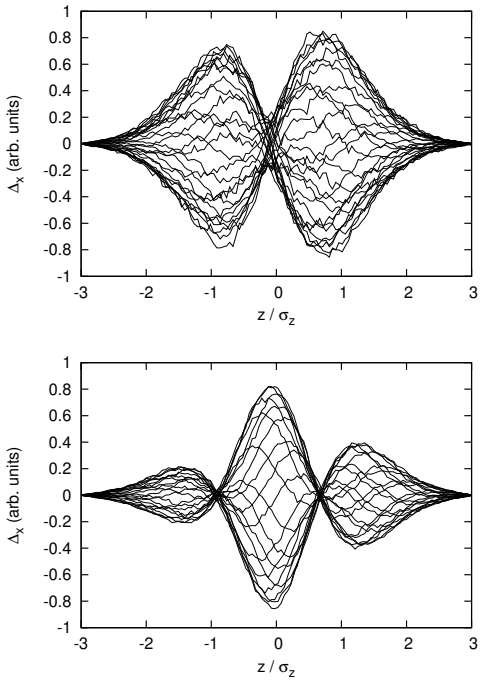

Figure 2: Examples for the unstable higher-order head-tail modes. Transverse offset traces along the bunch representing the $k = 1$ head-tail mode (top plot) and the $k = 2$ head-tail mode (bottom plot).

rate from a simulation without any damping for the $k = 0$ mode is $\Gamma = 1.1{\times}10^{-3}$, for the $k = 1$ mode it is $\Gamma = 7{\times}10^{-3}$, and for the $k = 2$ mode $\Gamma = 6 \times 10^{-3}$.

The method of our stability study implies finding the threshold octupole powers (both polarities) of the stability for a fixed space-charge condition. Figure 3 illustrates a simulation scan for $q = 2$ for the $k = 0$ mode. For the octupoles with $q_4 > 0.08$ and for the octupoles with $q_4 < -0.1$ the mode is stabilized, which are determined as the thresholds. The simulation runs are 10^4 turns long, which should provide the resolution for the growth rate well below $\Gamma = 10^{-4}$.

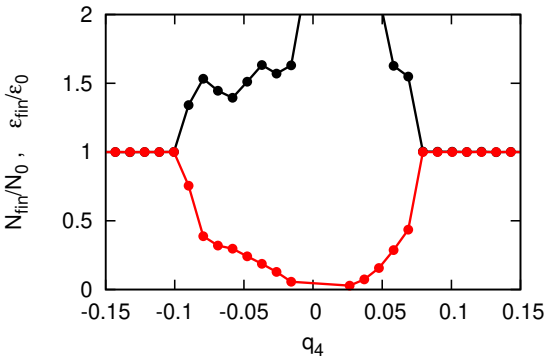

Figure 3: Output of an octupole power scan from simulations with space-charge ($q = 2$) for the unstable $k = 0$ modes. The red dots show the number of particles remained in the bunch, the black dots show the final horizontal emittance.

A stable (red lines) and an unstable (black lines) examples from simulations with octupoles and space-charge are shown in Fig. 4. The beam losses, the bunch horizontal offset and the bunch transverse emittance should be analized. Due to a strong dependency of the effective octupole from the transverse emittance, there can be a stabilizing emittance blowup [11]. In the situation with space-charge it is more complicated, because an emittance blowup also weakens space-charge.

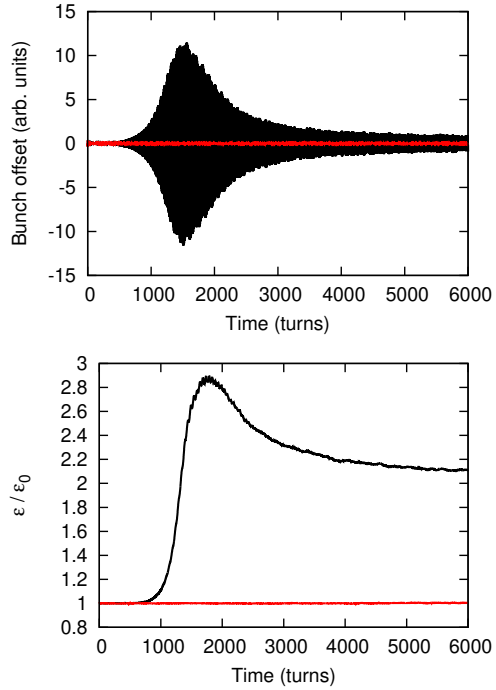

Figure 4: Time evolution of the bunch offset (top plot) and the transverse emittance (bottom plot) from simulations with octupoles and with space-charge ($q = 2$). The black lines correspond to $q_4 = 0.048$, the red lines are for $q_4 = 0.1$.

Results of the stability studies for the $k = 0$ mode are summarized in Fig. 5. The circles show the stability thresholds in the octupole power for the positive octupole polarity, the squares show the stability thresholds for the negative octupole polarity. The driving wake and the bunch parameters besides q are fixed. Thus, in this scan the increasing space-charge parameter q does not correspond to the increasing beam intensity, because the driving wake is not changed. We study Landau damping of a fixed instability for different space-charge conditions. Figure 6 shows the corresponding results for the $k = 1$ mode (top plot) and for the $k = 2$ mode (bottom plot).

DISCUSSION

The simulation results in Figs. 5, 6 suggest that more octupole power is needed for stability at stronger space-charge. This is similar to the loss of Landau damping due to linear space-charge in coasting beams. The incoherent tune distributions in Figs. 7–9 illustrate how space-charge shifts

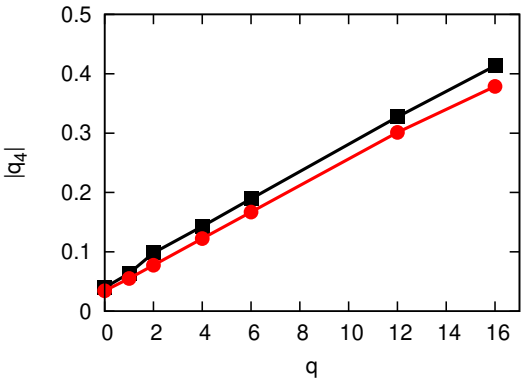

Figure 5: Results of the simulations scans for the $k = 0$ mode: stability thresholds in the octupole power in a dependency from the space-charge parameter q. The red circles are for the octupole polarity $q_4 > 0$, the black squares are for the octupole polarity $q_4 < 0$.

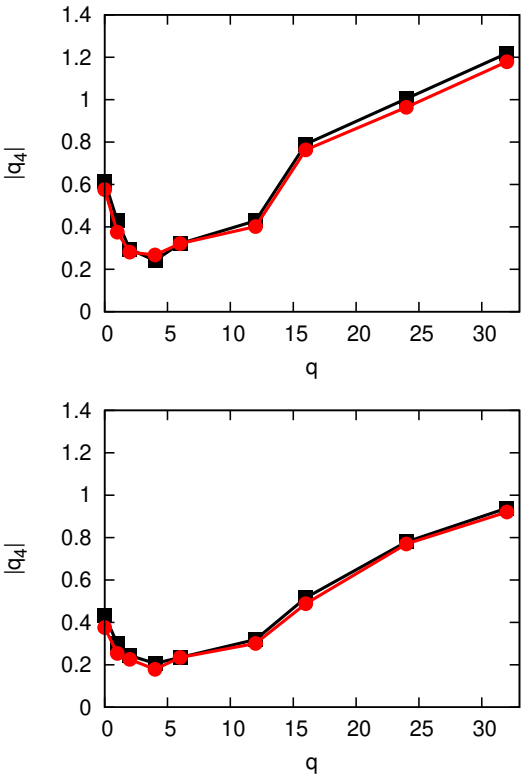

Figure 6: Results of the simulations scans for the $k = 1$ mode (top plot) and for the $k = 2$ mode (bottom plot). The plot notation corresponds to Fig. 5.

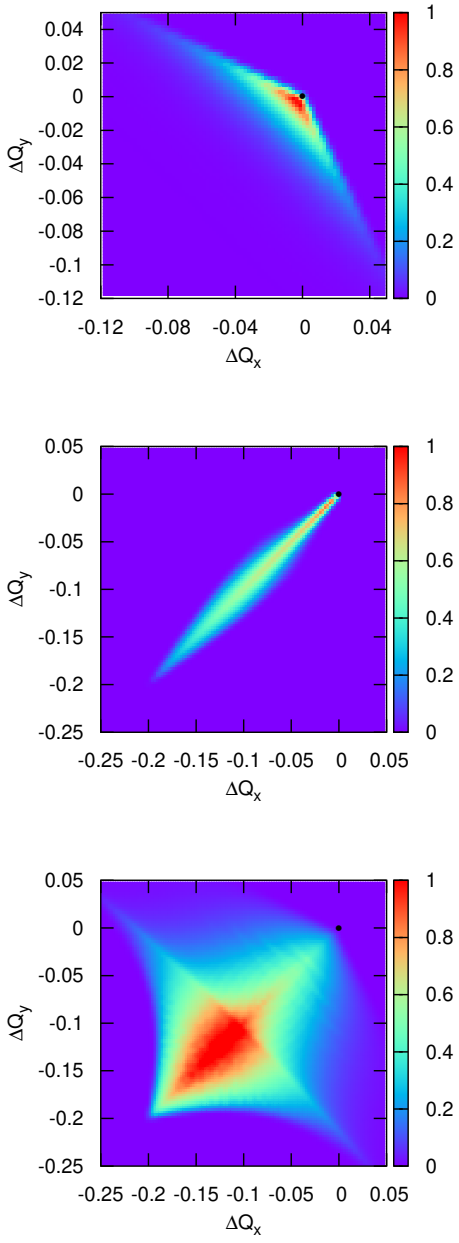

Figure 7: Tune footprints in a Gaussian bunch for the tune shifts due to octupoles $q_4 = 0.8$ (top plot), due to space-charge $q = 10$ (central plot) and for the combined effects (bottom plot). The color indicates the distribution density in arb. units, $Q_s = 0.01$.

particle tunes away from the bare tunes. Octupoles provide a tune spread, but the combined distribution is still strongly shifted. As a result, more octupole power is needed to provide enough tune spread. The coherent tune shifts of the instabilities are negative, in absolute value equal to the growth rate, which is a property of the resistive-wall wake [25]. In our case these values are below 0.01 in modulus. These tune shifts are small compared to the incoherent tune shifts, see Figs. 7–9.

Another observation from the results in Figs. 5, 6 is the "pits" in the q_4-growth for the $k = 1, 2$ modes at medium space-charge $q \lesssim 16$. This is in agreement with the findings about Landau damping due to space charge in bunches [19–23], for example, see Fig. 3 in [22]. In strong contrast, there is no "pit" in the results for the $k = 0$ mode (Fig. 5). This supports the conclusions [22, 23] that there is no additional

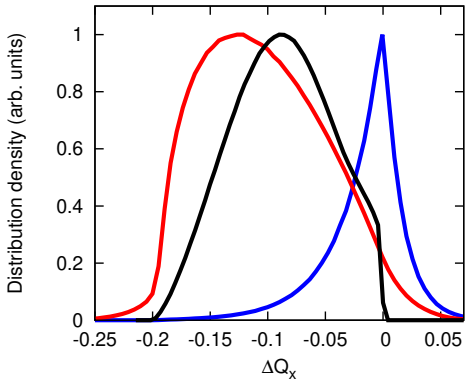

Figure 8: Incoherent tune distribution densities in a Gaussian bunch for the tune shifts due to octupoles $q_4 = 0.8$ (blue line), due to space-charge $q = 10$ (black line) and for the combined effects (red line), $Q_s = 0.01$.

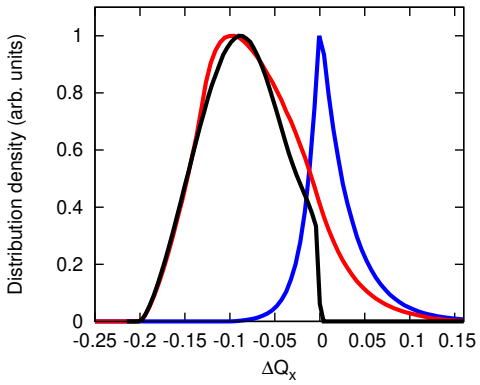

Figure 9: Incoherent tune distribution densities in a Gaussian bunch for the tune shifts due to octupoles $q_4 = -0.8$ (blue line), due to space-charge $q = 10$ (black line) and for the combined effects (red line), $Q_s = 0.01$.

Landau damping due to direct space-charge for the $k = 0$ mode.

Comparing the tune spreads due to octupoles of different polarity (blue lines in Figs. 8, 9), the related asymmetry is visible. This converts to the stability properties and can be analized using Eq. (6) or has also been observed in experiments [9]. Our results suggest that there are asymmetries for different octupole thresholds, see Fig. 3, and Figs. 5, 6. The polarity $q_4 > 0$ provides more damping and needs less octupole power for stability than that of $q_4 < 0$, especially at weak space-charge. For stronger space-charge, the differences in octupole thresholds (Figs. 5, 6) between octupole polarities are moderate. This corresponds to moderate differences for the combined space-charge and octupole effects in the tune destributions (red lines in Figs. 8, 9).

REFERENCES

[1] P. Spiller *et al.*, Proc. of IPAC2015, Richmond, VA, USA, May 2015, paper THPF015, p. 3715

[2] P. Spiller *et al.*, Proc. of IPAC2018, Vancouver, Canada, April-May 2018, paper MOZGBF2, p. 63

[3] J. Gareyte, J.P. Koutchouk and F. Ruggiero, CERN-LHC-Project-Report-91 (1997)

[4] V. Kornilov, O. Boine-Frankenheim, V. Kapin, Proc. of IPAC2010, Kyoto, Japan, May 23-28, p. 1988 (2010)

[5] F. Sacherer, Proc. First Int. School of Particle Accelerators, Erice, p. 198, CERN-PS-BR-76-21 (1976)

[6] I.M. Kapchinsky and V.V. Vladimirsky, In Proc. of the II. Int. Conf. on High Energy Accel., 1959.

[7] J.S. Berg, F. Ruggiero, CERN SL-AP-96-71 (1996).

[8] J.S. Berg, F. Ruggiero, Proc. of PAC1997, Vancouver, Canada, May 12-16, p. 1712 (1997)

[9] X. Buffat, W. Herr, N. Monet, T. Pieloni, S. White, Phys. Rev. ST Accel. Beams **17**, 111002 (2014).

[10] Y.-H. Chin, CERN/SPS/85-09 (1985)

[11] V. Kornilov, O. Boine-Frankenheim, Nuclear Inst. and Methods in Physics Research, A 951 (2020) 163042

[12] D. Möhl, H. Schönauer, Proc. IX Int. Conf. High Energy Acc., Stanford, 1974, p. 380 (1974)

[13] D. Möhl, CERN/PS 95-08 (DI), (1995)

[14] M. Blaskiewicz, Phys. Rev. ST Accel. Beams **4**, 044202 (2001)

[15] E. Métral, F. Ruggiero, Proc. EPAC2004, Lucerne, Switzerland, 5-9 July 2004, p. 1897 (2004)

[16] V. Kornilov, O. Boine-Frankenheim, and I. Hofmann, Phys. Rev. ST Accel. Beams **11**, 014201 (2008)

[17] A. Burov and V. Lebedev, Phys. Rev. ST Accel. Beams **12**, 034201 (2009)

[18] D.V. Pestrikov, Nuclear Inst. and Methods in Physics Research, A 562 (2006) 65-75

[19] A. Burov, Phys. Rev. ST Accel. Beams **12**, 044202 (2009); A. Burov, Phys. Rev. ST Accel. Beams **12**, 109901(E) (2009)

[20] V. Balbekov, Phys. Rev. ST Accel. Beams **12**, 124402 (2009)

[21] A. Macridin, A. Burov, E. Stern, J. Amundson, P. Spentzouris, Phys. Rev. ST Accel. Beams **18**, 074401 (2015)

[22] V. Kornilov and O. Boine-Frankenheim, Phys. Rev. ST Accel. Beams **13**, 114201 (2010)

[23] V. Kornilov and O. Boine-Frankenheim, arXiv:1709.01425 [physics.acc-ph] (2017)

[24] O. Boine-Frankenheim, V. Kornilov, Proc. of 9th International Computational Accelerator Physics Conference ICAP2006, Chamonix, France, Oct. 2-6, p. 267 (2006)

[25] V. Kornilov and O. Boine-Frankenheim, Proc. of 10th International Computational Accelerator Physics Conference ICAP2009, San Francisco, USA, Aug 31 - Sep 4, p. 58 (2009)

[26] I. Karpov, V. Kornilov, O. Boine-Frankenheim, Phys. Rev. Accel. Beams **19**, 124201 (2016)

[27] K. Blasche and B. Franczak, Proc. of EPAC1992, Berlin, Germany, March 24-28, p. 9 (1992)